

Ground-state properties of the disordered Hubbard model in two dimensionsMaria Elisabetta Pezzoli^{1,2} and Federico Becca^{2,3}¹*Department of Physics, Rutgers University, Piscataway, New Jersey 08854, USA*²*International School for Advanced Studies (SISSA), Via Beirut 2, I-34014 Trieste, Italy*³*CNR-IOM-Democritos National Simulation Centre, Trieste, Italy*

(Received 29 June 2009; published 5 February 2010)

We study the interplay between electron correlation and disorder in the two-dimensional Hubbard model at half filling by means of a variational wave function that can interpolate between Anderson and Mott insulators. We give a detailed description of our improved variational state and explain how the physics of the Anderson-Mott transition can be inferred from equal-time correlations functions, which can be easily computed within the variational Monte Carlo scheme. The ground-state phase diagram is worked out in both the paramagnetic and the magnetic sector. Whereas in the former a direct second-order Anderson-Mott transition is obtained, when magnetism is allowed variationally, we find evidence for the formation of local magnetic moments that order before the Mott transition. Although the localization length increases before the Mott transition, we have no evidence for the stabilization of a true metallic phase. The effect of a frustrating next-nearest-neighbor hopping t' is also studied in some detail. In particular, we show that t' has two primary effects. The first one is the narrowing of the stability region of the magnetic Anderson insulator, also leading to a first-order magnetic transition. The second and most important effect of a frustrating hopping term is the development of a “glassy” phase at strong couplings, where many paramagnetic states, with disordered local moments, may be stabilized.

DOI: [10.1103/PhysRevB.81.075106](https://doi.org/10.1103/PhysRevB.81.075106)

PACS number(s): 71.30.+h, 71.27.+a, 71.55.Jv

I. INTRODUCTION

Within independent-electron approaches, all single-particle states are delocalized and the metallic or insulating behavior is determined by the existence of an energy gap between the highest occupied level and the lowest unoccupied one. However, whenever the Coulomb interaction becomes dominant over the kinetic energy, the independent-electron picture fails and electrons in the narrow bands close to the Fermi energy become localized. Systems, whose insulating character is induced by electron correlations, are called *Mott insulators*.¹ The presence of disorder weakens the constructive interference that allows a wave packet to propagate coherently in a periodic potential and may eventually lead to single-particle localization at the Fermi energy, hence to a further class of insulating materials, called *Anderson insulators*.² In this context, the conventional one-parameter scaling theory of conductance³ predicts that all solutions of the single-particle Schrödinger equation in a disordered potential are localized in two dimensions (2D). Therefore, any amount of disorder in 2D drives a noninteracting electron system into an Anderson insulator. The inclusion of electron-electron interaction in weak coupling does not modify qualitatively the above conclusion,⁴ although it may crucially affect physical properties such as the tunneling density of states (DOS).^{4,5} Hence, it is widely accepted that 2D electron systems should always display an insulating behavior at sufficiently low temperature or large size no matter how weak the disorder is.

Nevertheless, from time to time some indications have appeared that this conclusion might not be always correct. Finkel'stein⁶ and Castellani *et al.*⁷ considered the interplay between disorder and interaction by perturbative renormalization group methods and showed that, for weak disorder

and sufficiently strong interactions, a 2D system might scale toward a phase with finite conductivity. However, this result was not conclusive since the “metallic” region is found to occur outside the theory's limits of validity. Indeed, the common feature of these calculations is the crucial role played by spin fluctuations that grow large as the renormalization procedure is iterated. This tendency has been commonly interpreted as the emergence of local moments concomitantly with the progressive Anderson localization and, in continuum systems, it might signal an incipient ferromagnetic instability.⁸ In lattice models, this is likely to be substituted by a magnetic instability at some wave vector determined by the topology of the Fermi surface. In this respect, an alternative approach could be to assume from the beginning a strong interaction that drives the system into a local moment regime, e.g., close to a magnetic Mott transition, and then turn on disorder. However, since it is already difficult to obtain an accurate description of a clean Mott transition, this approach is very hard to pursue. Moreover, assuming the scenario provided by dynamical mean-field theory (DMFT),⁹ one would immediately face with the so-called Harris criterion.¹⁰ Indeed, the correlation-length exponent predicted within DMFT for a clean Mott transition $\nu \approx 1/2$ is smaller than $2/D=1$ in $D=2$ dimensions.^{11,12} This fact implies that the whole critical behavior has to be profoundly altered by disorder, which therefore cannot be regarded at all as a weak perturbation.

Only with the groundbreaking experimental work by Kravchenko *et al.*,^{13,14} the statement that localization always occurs in 2D was really put into question. In fact, Kravchenko has been the first to observe and claim that, above some critical carrier density, high-mobility silicon metal-oxide-semiconductor field-effect transistors display a metallic behavior, i.e., a resistivity that decreases with decreasing temperature down to the lowest accessible one. Be-

low this critical density, the behavior of the resistance looks insulating, thus suggesting that a metal-insulator transition does occur by varying the density. This experimental finding has renewed the interest in the interplay between disorder and interaction and has generated further theoretical works along the same direction originally put forward by Finkel'stein, in the attempt to clarify some open issues and the applicability of the approach.^{15,16} However, the issue of having a genuine metallic phases in 2D is controversial and remains under debate from both the experimental and the theoretical point of view.¹⁷⁻¹⁹

An approach where neither the interaction nor the disorder are treated as a perturbation is therefore required to understand the complex physics of correlated disordered systems. The simplest model which contains both ingredients on the same level is the disordered Hubbard model, which has been intensively studied by several numerical methods, such as Hartree-Fock calculations in two²⁰ and three dimensions,^{21,22} extended DMFT,²³⁻²⁸ and quantum Monte Carlo simulations.²⁹⁻³² However, all these methods have some drawback and only a combined analysis of complementary techniques can be able to clarify the nature of this challenging problem. Any approach based on single-particle descriptions, such as unrestricted Hartree-Fock,^{20,33} can uncover the emergence of an insulating gap only by forcing magnetic long-range order. More sophisticated approaches, like those based on DMFT,^{23,24} can, in principle, manage without magnetism,^{25,26,34,35} but they usually miss important spatial correlations. The spatial distribution of local moments and its connection with Griffiths singularities, which may emerge close to the Mott insulator,³⁶ have been recently discussed within a Brinkmann-Rice approach of the Gutzwiller wave function.³⁷

In Ref. 38, an improved approach based on a variational wave function has been proposed to deal simultaneously with the physics of Anderson's and Mott's localization. In this work, we present an extensive and more complete study of the ground-state properties of the disordered Hubbard model in two dimensions at half filling. Moreover, we also discuss in great details the variational method used in our calculations. Within our approach it is possible to describe both a direct transition between a compressible Anderson insulator and an incompressible paramagnetic Mott phase and a transition to a magnetically ordered insulator. In the first part, we discuss the variational wave function and we explain how it is possible to distinguish between Anderson and Mott insulators, by means of static correlation functions. In the second part, we describe paramagnetic and magnetic transitions. By allowing for magnetic order, we show the evidence for the formation of local magnetic moments that order *before* the Mott transition. Finally, we introduce a frustrating (next-nearest-neighbor) hopping that favors a glassy behavior with many different local minima (and presumably long time scales).

The paper is organized as follows: in Sec. II we present the method and the variational wave function that is used in our calculations; in Sec. III we show the accuracy of our method; in Sec. IV we show our numerical results for the paramagnetic sector; in Sec. V we present the results for the magnetic sector; finally, in Sec. VI we draw our conclusions.

II. MODEL AND METHODS

A. Variational wave function

We consider the two-dimensional Hubbard model with on-site disorder

$$\mathcal{H} = - \sum_{i,j,\sigma} t_{ij} c_{i,\sigma}^\dagger c_{j,\sigma} + \text{H.c.} + \sum_i \epsilon_i n_i + U \sum_i n_{i,\uparrow} n_{i,\downarrow}, \quad (1)$$

where $c_{i,\sigma}^\dagger$ ($c_{i,\sigma}$) creates (destroys) an electron at site i with spin σ , and $n_i = \sum_\sigma n_{i,\sigma}$ is the local density operator. ϵ_i are random on-site energies chosen independently at each site i and uniformly distributed between $[-D, D]$, U is the repulsive electron-electron interaction and t_{ij} is the hopping amplitude. In the first part of this work, we consider only a nearest-neighbor hopping term $t=1$ and, in the final part, we also add a frustrating next-nearest-neighbor term t' . We consider 45° rotated clusters with $N=2l^2$ sites at half filling, i.e., with $N_e=N$ electrons.

For $U=0$, the Hamiltonian (1) reduces to the Anderson model for which the ground state is an Anderson insulator for any value of D , with gapless charge excitation but localized states. On the contrary, in the opposite limit $U/t \rightarrow \infty$, all charge fluctuations are suppressed, the system recovers translational invariance and the ground state becomes a Mott insulator. In this work, we study the zero-temperature properties for finite disorder D and Coulomb interaction U , by using the variational Monte Carlo algorithm. Our variational ansatz for the ground state is given by

$$|\Psi\rangle = \mathcal{JG}|SD\rangle, \quad (2)$$

where $|SD\rangle$ is an uncorrelated Slater determinant that is the ground state of a mean-field Hamiltonian

$$\mathcal{H}_{MF} = - \sum_{i,j,\sigma} \tilde{t}_{ij} c_{i,\sigma}^\dagger c_{j,\sigma} + \text{H.c.} + \sum_{i,\sigma} \tilde{\epsilon}_{i,\sigma} n_{i,\sigma}, \quad (3)$$

where $\tilde{t}_{ij}=t$ for neighboring sites and $\tilde{\epsilon}_{i,\sigma}$ are variational parameters; in addition the next-nearest-neighbor hopping $\tilde{t}_{ij}=\tilde{t}'$ is also used as a variational parameter in case of a finite value of t' in the Hamiltonian. We consider both paramagnetic and magnetic properties. In the former case, we impose the wave function $|\Psi\rangle$ to be paramagnetic, by fixing the variational parameters $\tilde{\epsilon}_{i,\downarrow}=\tilde{\epsilon}_{i,\uparrow}$. On the contrary, in order to study magnetic properties, we consider a variational wave function that may break the spin-rotational symmetry, namely, we allow the variational parameters to be $\tilde{\epsilon}_{i,\downarrow} \neq \tilde{\epsilon}_{i,\uparrow}$.

A more general choice of the trial wave function could also contain additional parameters for all (nearest-neighbor) hopping terms \tilde{t}_{ij} (with no translational invariance). Calculations performed on small lattices showed that, despite a much larger computational effort, this ansatz leads only to slightly lower energies, without modifying the ground-state properties. Therefore, this possibility will be not considered in the following.

The Gutzwiller factor \mathcal{G} is defined by

$$\mathcal{G} = \exp \left[- \sum_i g_i m_i^2 \right] \quad (4)$$

and \mathcal{J} is a long-range Jastrow term, defined by

$$\mathcal{J} = \exp \left[-\frac{1}{2} \sum_{i,j} v_{ij} (n_i - 1)(n_j - 1) \right]. \quad (5)$$

While the Gutzwiller factors have been defined with a different parameter g_i for each site in order to describe the nonhomogeneous character of the system, we only consider translational invariant $v_{i,j} = v(|r_i - r_j|)$. In the following, the Fourier transform of the Jastrow parameters will be denoted by v_q . All these parameters can be optimized in order to minimize the variational energy. The choice of taking translational invariant $v_{i,j}$ is done in order to reduce the total number of parameters and make the problem tractable from a numerical point of view. Moreover, since the Jastrow factor plays a primary role in the strong-coupling regime, where the disorder effects are suppressed, this choice should not put serious limitations to our variational wave function.

Summarizing, the variational parameters are (i) the on-site energies $\tilde{\epsilon}_{i,\sigma}$ and, for $t' \neq 0$ the hopping \tilde{t}' of the mean-field Hamiltonian (3), (ii) the Gutzwiller parameters g_i , and (iii) the translational invariant Jastrow parameters $v_{i,j}$. The optimization of the variational state, without assuming any particular parametric form, is done by an energy minimization, which may deal with a large number (few hundreds) of parameters.³⁹

B. Correlation functions

To work out the zero-temperature phase diagram, we make use of the f-sum rule that allows us to interpret the small- q behavior of density-density correlations. Starting from the definition of the average energy of the excitations

$$\Delta_q = \frac{\int d\omega \omega N_q(\omega)}{\int d\omega N_q(\omega)}, \quad (6)$$

where $N_q(\omega)$ is the dynamical structure factor. By integrating over frequencies this quantity, we obtain the static structure factor N_q

$$N_q = \int \frac{d\omega}{2\pi} N_q(\omega). \quad (7)$$

We emphasize that N_q can be easily calculated within the Monte Carlo method through an equal-time density-density correlation over the ground state

$$N_q = \overline{\langle n_{-q} n_q \rangle} - N_q^{\text{disc}}, \quad (8)$$

where $\langle n_{-q} n_q \rangle = \langle \Psi | n_{-q} n_q | \Psi \rangle$ indicates the quantum average and the overbar denotes the disorder average. Notice that, in order to have a correct definition of the dynamical structure factor $N_q(\omega)$, we have subtracted the disconnected term

$$N_q^{\text{disc}} = \overline{\langle n_{-q} \rangle \langle n_q \rangle}, \quad (9)$$

which is related to the elastic scattering of electrons and, in a disordered system, is finite for generic momenta q .⁴⁰ Notice that, in a disordered system q is no longer a good quantum number but, nevertheless, the average over different disorder configurations restores the translational invariance. This fact suggests that the density-density structure factor N_q can be a meaningful quantity to assess physical properties.

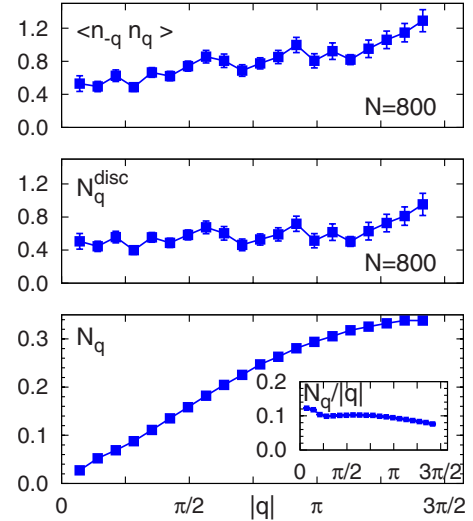


FIG. 1. (Color online) Density-density correlation function $\langle n_{-q} n_q \rangle$ (upper panel), disconnected term N_q^{disc} (middle panel), and $N_q = \langle n_{-q} n_q \rangle - N_q^{\text{disc}}$ (lower panel) for the noninteracting Anderson insulator. The inset shows $N_q/|q|$, from which it is clear that $N_q \sim |q|$. Results are averaged over 48 disorder realizations with $D/t=5$ for $N=800$ sites.

After a straightforward calculation, we arrive to a simple expression of Δ_q for small momenta

$$\lim_{q \rightarrow 0} \Delta_q \sim \frac{q^2}{N_q}. \quad (10)$$

From this equation, we have the important result that $N_q \sim |q|$ implies the existence of gapless charge modes, since $\Delta_q \rightarrow 0$ for $|q| \rightarrow 0$, while if $N_q \sim q^2$ charge excitations are presumably gapped, since $\Delta_q \sim \text{const}$ for $|q| \rightarrow 0$. These criteria have been already applied with success to the fermionic and bosonic Hubbard models without disorder,^{41,42} where it has been demonstrated that it is possible to describe a true Mott insulator by using a Jastrow-Slater wave function. In addition, it has been shown that there is a tight connection between N_q and the Jastrow parameters v_q . For a clean system, a conducting state (metallic or superconducting in the fermionic case and superfluid in the bosonic one) is characterized by $v_q \sim 1/|q|$ in any spatial dimensions, whereas, in order to correctly reproduce the static structure factor of a Mott insulator, v_q must be more singular, i.e., $v_q \sim 1/q^2$ in one and two dimensions and $v_q \sim 1/|q|^3$ in three dimensions.⁴¹

Let us now turn to the disordered model. Before considering the interacting case, we would like to discuss the results for the noninteracting case and show that $N_q \sim |q|$ is recovered, in agreement with the fact that the ground state is compressible. In Fig. 1, we report the density-density correlations $\langle n_{-q} n_q \rangle$ and the disconnected term N_q^{disc} calculated for a system with $N=800$ sites and disorder strength $D/t=5$, averaged over 48 disorder realizations. It is clear that both quantities are finite for $q \rightarrow 0$. However, once we consider the connected part of the density-density correlations N_q , we have that $N_q \sim |q|$ for $q \rightarrow 0$, in agreement with the fact that

the Anderson insulator is gapless, see Fig. 1. We would like to emphasize that, in contrast to the clean case where $N_q \sim |q|$ implies a conducting behavior, here it just indicates a compressible state with gapless excitations, but not a metallic character, because the single-particle states are localized.

III. ACCURACY OF THE WAVE FUNCTION

The variational energy landscape of the disordered Hubbard model may be characterized by the presence of different local minima. In fact, if we start from different points in the parameter space, namely, from different values of g_i , $v_{i,j}$, and $\tilde{\epsilon}_{i,\sigma}$, we may converge to different solutions. In the following, whenever we consider the paramagnetic sector, we impose $\tilde{\epsilon}_{i,\uparrow} = \tilde{\epsilon}_{i,\downarrow}$ along the whole optimization procedure. On the other hand, when magnetic solutions are allowed, these conditions are relaxed along the Monte Carlo simulation and the two on-site energies (for up and down spins) are optimized independently. In the latter case, the starting configuration can be taken to be either paramagnetic (i.e., with $\tilde{\epsilon}_{i,\uparrow} = \tilde{\epsilon}_{i,\downarrow}$) or with a small staggering of the magnetization [i.e., with $\tilde{\epsilon}_{i,\sigma} = \tilde{\epsilon}_i + \sigma(-1)^{|x_i+y_i|} \delta$, where δ is a small quantity]. We would like to stress that, even by considering a paramagnetic starting point, the converged solution will generally have $\tilde{\epsilon}_{i,\uparrow} \neq \tilde{\epsilon}_{i,\downarrow}$.

In contrast to the paramagnetic case, in which the energy landscape usually has one minimum (i.e., the same parameters are obtained when starting from different initializations), when allowing a magnetic wave function different local minima may appear. This feature is particularly evident for large enough Coulomb repulsion, whereas in the weak-coupling regime we recover a simple picture with only one minimum. Remarkably, the appearance of different local minima is related to the presence of short-range magnetic correlations. In fact, by increasing the on-site Coulomb repulsion, some sites acquire a finite magnetization and eventually order, giving rise to the typical staggered pattern. Whenever local moments are present or the magnetization is very small, there are different electronic arrangements that give similar energies but may be hardly connected by simple single-particle moves, so to define metastable local minima. However, especially for the unfrustrated or the weakly frustrated case, the presence of these local minima is not a dramatic problem. In fact, generally, all physical quantities, as, for instance, the density-density structure factor N_q , give similar results in all these cases. Therefore, we can safely conclude that all the optimized states share the same physical properties. As an example, Fig. 2 shows the on-site magnetization $\langle m_i \rangle = \langle n_{i,\uparrow} - n_{i,\downarrow} \rangle$ pattern for the variational wave function optimized both starting from the paramagnetic point and from the staggered point. It is evident that there is no considerable difference between the two states, although some of the magnetization values are slightly different.

We remark that, in most cases, we obtain a lower variational energy by starting from the paramagnetic point, even if the final converged state is magnetically ordered. Therefore, although in some particularly delicate cases we considered different starting points, we usually initialize the simulation with a paramagnetic configuration.

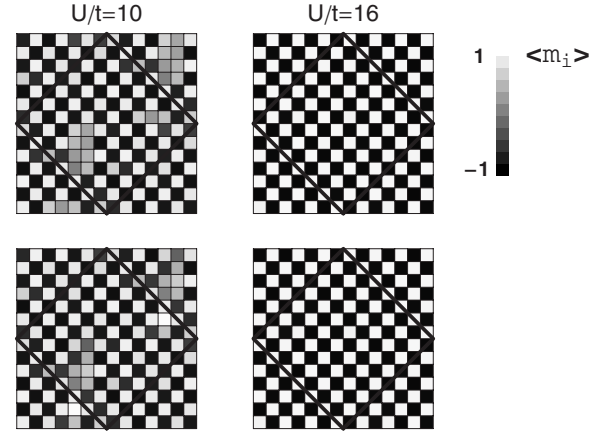


FIG. 2. On-site magnetization $\langle m_i \rangle$ for a typical disorder configuration with $D/t=5$, $U/t=10$ (left panels) and $U/t=16$ (right panels). The upper panels correspond to the wave function obtained starting from a paramagnetic point, whereas the lower panels correspond to the solution obtained from a staggered point. The black contour shows the elementary cell of the lattice which is repeated to mimic the infinite lattice with periodic boundary conditions.

Let us now discuss the accuracy in energy for a 4×4 lattice, where the exact ground state can be calculated exactly by the Lanczos algorithm. In particular, we consider four different wave functions: (i) the magnetic state with on-site Gutzwiller and Jastrow factors (that corresponds to our best ansatz), (ii) the paramagnetic state with Gutzwiller and Jastrow terms, (iii) the magnetic state with only Gutzwiller projectors, and (iv) the magnetic mean-field state $|SD\rangle$ (i.e., without any correlation term). For $U=0$, the exact ground-state wave function can be obtained in all these cases, implying a very good accuracy also for small but finite values of U/t . For small interactions there is no appreciable differences between paramagnetic and magnetic wave functions and for all *correlated* states the accuracy in the energy, i.e., $(E_0 - E_v)/E_0$ (where E_0 and E_v are the exact and the variational energies, respectively) is lower than 1%. However, even for $U/t=4$, the Hartree-Fock state, with no Gutzwiller and Jastrow factors, give a much worse accuracy than the other three correlated wave functions, see Fig. 3. For larger values of the interaction U , the situation is different, since the paramagnetic state is generally worse than the magnetic wave functions, including the Hartree-Fock state. The accuracy of our best ansatz is about 10% (or less) up to very large Coulomb repulsions, which is acceptable in a disordered model. However, we notice that the long-range Jastrow factor is not crucial, and wave functions (i) and (iii) give comparable energies both for small and large interaction values, e.g., $U/t=4$ and 16, see Fig. 3. In fact, on the one hand, the on-site Gutzwiller factor can easily account for the small charge correlations induced by the Coulomb repulsion in the weak-coupling regime. On the other hand, for large U/t , the ground state has strong magnetic correlations and is well described with a (gapped) mean-field state. In the intermediate regime, our magnetic state with both on-site Gutzwiller projectors and the long-range Jastrow term may give a considerable improvement over the other states considered here. It should be stressed, however, that the Jastrow factor is es-

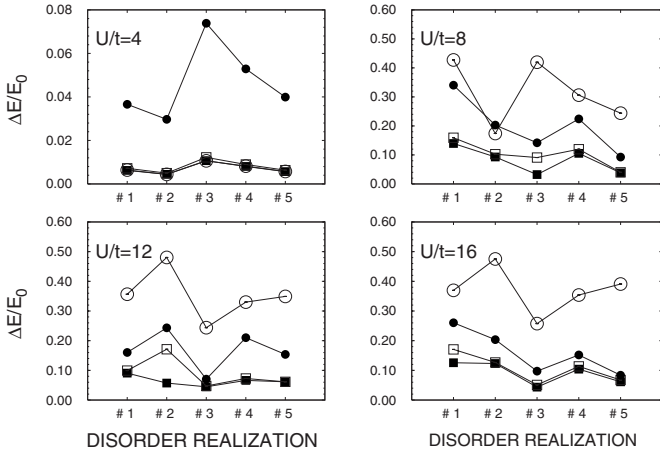


FIG. 3. Accuracy of the variational energies $\Delta E = (E_0 - E_v)$ (where E_0 and E_v are the exact and the variational energies, respectively) for different wave functions on a 4×4 lattice with $D/t=5$: the correlated magnetic state (full squares), the paramagnetic state (empty circles), the magnetic state without Jastrow factors (empty squares), and the Hartree-Fock state (full circles). The exact ground-state energy is computed by the Lanczos algorithm.

sential to have a *paramagnetic* Mott insulator, since in this case the charge gap cannot be opened by an uncorrelated Hartree-Fock state. On the contrary, in the magnetic case, long-range Jastrow correlations are not strictly necessary to capture the correct nature of the ground state, since the charge gap can be naturally created by a finite antiferromagnetic mean-field parameter.

IV. RESULTS: THE PARAMAGNETIC CASE

Let us start our analysis of the disordered Hubbard Hamiltonian (1) by enforcing a paramagnetic variational wave function, e.g., by fixing the constraint $\tilde{\epsilon}_{i,\uparrow} = \tilde{\epsilon}_{i,\downarrow}$ for the parameters of the auxiliary mean-field Hamiltonian (3). Although this choice is biased, since antiferromagnetic order may be present for finite electron-electron interaction, it gives significant insights into the interplay between disorder and interaction, without any “spurious” effect due to magnetism. We apply the f-sum rule to distinguish the compressible Anderson insulator from the incompressible Mott insulator, i.e., we look at the different behavior of N_q and v_q for different values of interaction U and disorder D . Here, we take a rather strong disorder ($D/t=4, 5$, and 6) in order to have a localization length that is smaller than the numerically accessible system sizes.

A detailed analysis of these quantities allows us to identify the Mott transition at $U_c^{\text{MI}} = (11.5 \pm 0.5)t$ for $D/t=5$.³⁸ Indeed, for small values of the interaction strength, i.e., for $U < U_c^{\text{MI}}$, we have that $N_q \sim |q|$, whereas $N_q \sim q^2$ in the strong-coupling regime $U > U_c^{\text{MI}}$. The latter behavior is symptomatic of the presence of a charge gap hence of a Mott insulating behavior.⁴¹ We would like to emphasize that the present results are qualitatively similar to those obtained within the clean Hubbard model, with linear coefficient of N_q going smoothly to zero at the phase transition, indicating that the transition is likely to be continuous. We mention that the

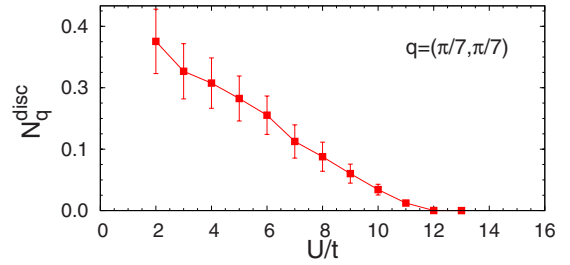


FIG. 4. (Color online) Disconnected part of the density-density correlation function N_q^{disc} for the smallest q as a function of the interaction U for $D/t=5$ and $N=98$ sites.

Fourier transform v_q of the optimized Jastrow parameters $v_{i,j}$ is also compatible with a Mott transition at the same value of the interaction strength, with its small- q behavior changing from $v_q \sim 1/|q|$ to $v_q \sim 1/q^2$ across the Mott transition.³⁸

Most interestingly we find that N_q^{disc} goes continuously to zero at the phase transition, see Fig. 4. This fact allows us to identify a simple and variationally accessible quantity to distinguish between an Anderson insulator and a Mott insulator. We would like to stress that this behavior is not restricted to $q \rightarrow 0$, but we recover a similar trend also for finite momenta, although disorder fluctuations are larger for larger q vectors, see Fig. 5. These results demonstrate that charge fluctuations are strongly suppressed and eventually become *local* as U/t increases.

All these results suggest that disorder is strongly suppressed in the regime of strong correlations. This fact is also corroborated by the calculation of the variance of the distribution of the on-site energies $\tilde{\epsilon}_{i,\sigma}$, which was shown in Ref. 38. Previous Monte Carlo calculations have shown that a repulsive interaction may screen the local energies, thereby generating an effectively weaker random potential.²⁹ At the mean-field level⁴³ and beyond,²⁴ the screening effects have been widely discussed. The Hartree-Fock state leads to a disorder screening only for moderate interactions, while it gives almost unscreened on-site energies in the strongly correlated regime. On the contrary, our correlated variational approach is able to capture the correct physics also for large interaction U , where the disorder, though finite, is highly suppressed. The redistribution of on-site energies leads to a decreased localization of the electronic state at the Fermi level. Nevertheless, the single-particle eigenstates are always

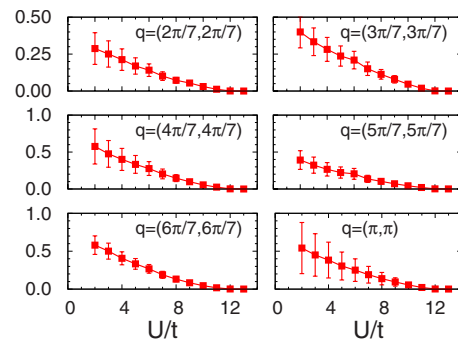


FIG. 5. (Color online) The same as in Fig. 4 for different momenta.

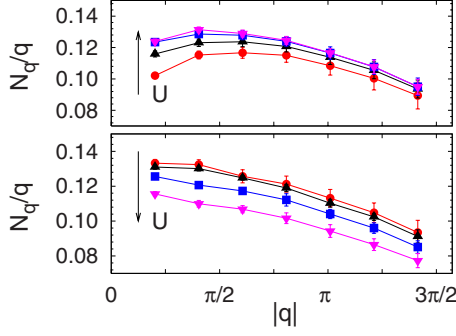


FIG. 6. (Color online) Static structure factor N_q divided by $|q|$ as a function of $|q|$ for different values of the interaction U . Upper panel: $U/t=2$ (circles), 3 (upward triangles), 4 (squares), and 5 (downward triangles). Lower panel: $U/t=6$ (circles), 7 (upward triangles), 8 (squares), and 9 (downward triangles). Calculations have been done for $D/t=5$ and $N=98$ sites.

localized, even though a very large localization length may develop. Within our variational approach, an important question is whether the action of the Gutzwiller correlator and the Jastrow factor could turn a localized $|SD\rangle$ into a delocalized many-body state $|\Psi\rangle$. Unfortunately, the variational method does not give access to dynamical quantities and, therefore, we cannot make a definite statement. Nevertheless, we tend to believe that such a transmutation of a localized $|SD\rangle$ into a delocalized $|\Psi\rangle$ is unlikely. In any case, the previous results show an increase in the “metallicity” of the ground state with a partial screening of disorder. This result is in agreement with the fact that the linear slope of N_q has a nonmonotonic behavior as a function of U , showing a peak for $U/t \sim 7$ that indicates an accumulation of low-energy states around the Fermi energy, see Fig. 6. In fact, the linear slope of N_q is related to the compressibility of the system. Nevertheless, it has to be noticed that the Slater determinant $|SD\rangle$ is the ground state of a mean-field Hamiltonian that always describes noninteracting electrons with on-site disorder, no matter how large the Coulomb repulsion is. Therefore, even though the single-particle eigenstates may have a very long localization length because of the suppression of the effective on-site disorder, yet this length remains finite in two dimensions.

The analysis of the density-density correlation function, the Jastrow factor and N_q^{disc} for different values of D/t allows us to draw the paramagnetic phase diagram in the (U, D) plane, see Fig. 7. Finally, in order to gain a deeper understanding on the local behavior, namely, how each single site behaves across the Anderson-Mott transition, we introduce a local f-sum rule

$$\Delta_j(q) = \frac{\Sigma_j(q)}{N_j(q)}. \quad (11)$$

Here $N_j(q)$ defines the local static structure factor

$$N_j(q) = \frac{1}{N} \sum_i \langle n_i n_j \rangle_{\text{conn}} e^{iq(R_i - R_j)}, \quad (12)$$

where $\langle n_i n_j \rangle_{\text{conn}}$ represents the quantum average of $n_i n_j$ after subtracting the disconnected term $\langle n_i \rangle \langle n_j \rangle$. In addition, $\Sigma_j(q)$ is related to the local kinetic energy

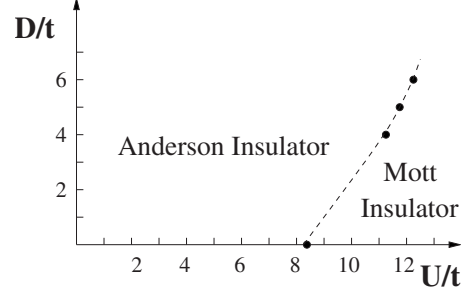


FIG. 7. Phase diagram for the disordered Hubbard model in the paramagnetic sector.

$$\Sigma_j(q) = -2t \sum_{\langle i,j \rangle \sigma} \langle c_{i,\sigma}^\dagger c_{j,\sigma} + \text{H.c.} \rangle (e^{iq(R_i - R_j)} - 1), \quad (13)$$

where $\langle i \rangle_j$ indicates the sum over the nearest neighbors of the site j . Both $\Sigma_j(q)$ and $N_j(q)$ can be easily evaluated in the variational Monte Carlo scheme, since they require the computation of equal-time correlations.

The limit for small momenta of Eq. (11) gives important insights into the local gap, making it possible to understand if at the Mott transition all sites become localized simultaneously, or nonhomogeneous fluctuations are still present. In Fig. 8, we report the distribution of $\Sigma_j(q)$, evaluated at the smallest value of the q available within a 98-site lattice, i.e., $q = (\pi/7, \pi/7)$. The average value of $\Sigma_j(q)$ slightly increases by increasing U and it has a maximum in the regime $U \sim D$ (similarly to what happens to $N_q/|q|$, see Fig. 6). The distribution $P[\Sigma_j(q)]$ is rather large for small U/t and shrinks when the interaction strength is increased, in agreement with the fact that disorder is suppressed by interaction. However, even very close to the Mott transition, the variance of $P[\Sigma_j(q)]$ stays quite large, indicating that a considerable number of sites still has large fluctuations. This fact can be interpreted as a two-fluid behavior, where a fraction of sites can be regarded as localized particles, whereas the remaining ones behave like in the Anderson insulator. Therefore, the Mott transition is driven by only a fraction of the total num-

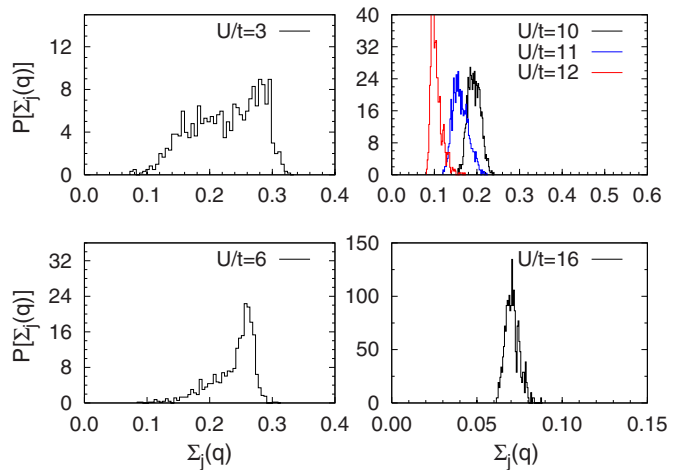


FIG. 8. (Color online) Distribution of $\Sigma_j(q)$ evaluated at $q = (\pi/7, \pi/7)$. Calculations are done for $D/t=5$ and $N=98$ sites.

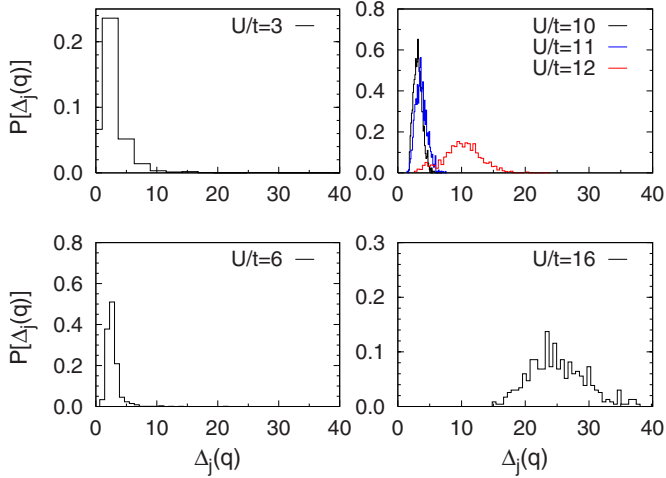


FIG. 9. (Color online) The same as in Fig. 8 but for the local gap $\Delta_j(q)$.

ber of sites. For $U > U_c^{\text{MI}}$, we recover a situation where all sites can be ascribed to the Mott phase and $P[\Sigma_j(q)]$ has a very sharp peak with a small variance. The distribution of $N_j(q)$ is very similar to the one of the local kinetic term. By contrast, the distribution of the local gap $\Delta_j(q)$ is rather narrow for $U < U_c^{\text{MI}}$, where for small momenta $\Delta_j(q) \sim 0$, due to a vanishing gap in the Anderson phase, see Fig. 9. Nevertheless, the distribution has very long tails (with very small weight), which are related to disorder fluctuations; these tails tend to be suppressed by increasing the interaction U . For $U > U_c^{\text{MI}}$, a charge gap opens up in the average density of states but the size of the gap turns out to be different from site to site, which implies a rather broad distribution, see Fig. 9.

V. RESULTS: THE MAGNETIC CASE

On the square lattice at half filling, in the absence of frustration and disorder, an arbitrarily weak repulsive Hubbard interaction U is able to induce long-range antiferromagnetic order. In fact, in this case, the presence of a perfect nesting in the Fermi surface implies a diverging susceptibility at $Q=(\pi, \pi)$ that, in turn, opens a finite gap at the Fermi level. Therefore, the ground state is a band insulator for any finite value of the interaction $U > 0$. By contrast, in the presence of a local random potential, the charge gap may be filled by (localized) energy levels, possibly destroying the long-range magnetic order. Here, we address the important problem of the competition between Anderson localization and magnetic order by using our improved variational approach and allowing for a magnetic Slater determinant $|\text{SD}\rangle$ with $\tilde{\epsilon}_{i,\downarrow} \neq \tilde{\epsilon}_{i,\uparrow}$. First, we discuss the phase diagram of the disordered Hubbard model in Eq. (1) with only a nearest-neighbor hopping t . In this case, a finite value of the interaction U_c^{AF} is needed to have the onset of long-range magnetic order: below U_c^{AF} the system is described by a standard paramagnetic (compressible) Anderson insulator, above U_c^{AF} a finite antiferromagnetic order parameter develops; however, the excitation spectrum remains gapless and the system

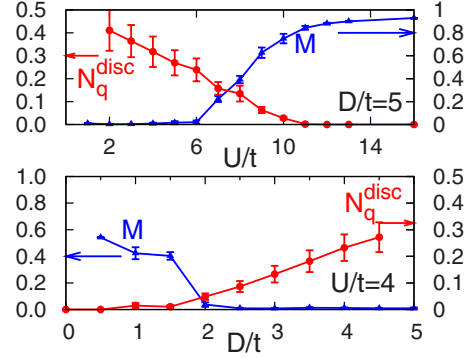


FIG. 10. (Color online) Staggered magnetization M and the disconnected term of the density-density correlations N_q^{disc} as a function of U for disorder $D/t=5$ (upper panel) and as a function of D for $U/t=4$ (bottom panel). All calculations have been done for $N=98$ sites.

is compressible. By further increasing the interaction U , i.e., for $U > U_c^{\text{MI}}$ the ground state undergoes a second phase transition to an incompressible antiferromagnetic insulator with a finite charge gap. Interestingly, in the paramagnetic Anderson insulator, local moments with a finite value of $\langle m_i \rangle = \langle n_{i,\uparrow} - n_{i,\downarrow} \rangle$ develop, suggesting that itinerant electrons may not be able to fully screen magnetic impurities created by disorder.

In the last part, we add a next-nearest-neighbor (frustrating) hopping t' . Also in this case, we show that the Mott insulating phase is always accompanied by magnetic order, although with a sufficiently large ratio t'/t many local minima appear in the energy landscape, with competing magnetic properties. In particular, we find that the lowest energy solution displays magnetic long-range order but many other disordered states with localized moments may be stabilized.

A. Magnetic phase diagram

Let us now consider large systems. In order to assess the magnetic properties, we define the total magnetization

$$M = \frac{1}{N} \sum_i e^{iqR_i} \langle m_i \rangle, \quad (14)$$

where $m_i = n_{i,\uparrow} - n_{i,\downarrow}$. In analogy with the clean model, also in presence of disorder, by increasing the electron-electron repulsion, there is a tendency toward magnetic order at $Q=(\pi, \pi)$, and, therefore, we concentrate on this value of the momentum.

In Fig. 10, we report our results for $D/t=5$ and different values of the Coulomb repulsion and for $U/t=4$ and various disorder strength. Fixing $D/t=5$, we find that $U_c^{\text{AF}} = (6.5 \pm 0.5)t$, since the magnetization is finite for $U > U_c^{\text{AF}}$ whereas it vanishes for $U < U_c^{\text{AF}}$. Moreover, as we discussed in the previous section, the information about charge fluctuations can be worked out from either N_q or the disconnected term N_q^{disc} . We obtain that N_q^{disc} vanishes at $U_c^{\text{MI}} = (10.5 \pm 0.5)t$, signaling the opening of a charge gap, see Fig. 10. Remarkably, there is a finite region in which both the

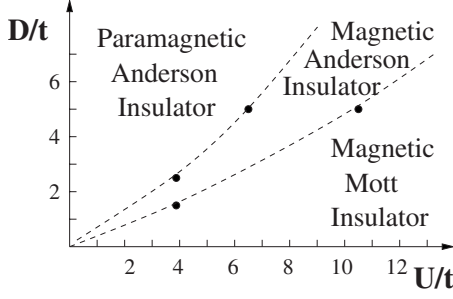


FIG. 11. Phase diagram for the disordered Hubbard model in the magnetic sector.

magnetization and the compressibility fluctuations are finite. This fact implies a stable regime that shows antiferromagnetic long-range order without a charge gap. We notice that this intermediate phase is much reduced when considering $U/t=4$ and vary the disorder strength, see Fig. 10. In this case, we can estimate that $D_c^{\text{AF}}=(2.5 \pm 0.5)t$ and $D_c^{\text{MI}}=(1.5 \pm 0.5)t$. These results lead to the phase diagram sketched in Fig. 11. For $U=0$ the system is a (paramagnetic) Anderson insulator for every finite disorder $D>0$. Instead, for $D=0$ the ground state is a Mott insulator with antiferromagnetic order for every $U>0$. When both disorder and interaction are finite, there is an intermediate phase between the paramagnetic Anderson insulator and the antiferromagnetic Mott insulator. This phase is characterized by long-range magnetic order but also by a finite compressibility. Although some authors identified this phase with a metal,²⁰ we do not find any evidence in favor of it (see below).

Let us now consider in more detail the nature of the Anderson-Mott transition that emerges from our variational approach, once we allow for spin-rotational symmetry breaking. We would like to remind the reader that, in the paramagnetic case, the Mott insulator can be obtained only thanks to a singular Jastrow factor, i.e., $v_q \sim 1/q^2$. In this case, the (paramagnetic) mean-field Hamiltonian (3) is always gapless and the charge gap opens because of the strong correlations induced by the Jastrow term. In the magnetic case instead, two different mechanisms can open a gap: (i) the long-range charge correlations induced by the Jastrow factor and (ii) the onset of long-range antiferromagnetic order due to a staggering of the $\tilde{\epsilon}_{i,\sigma}$'s. For $U < U_c^{\text{MI}} = (10.5 \pm 0.5)t$, the static structure factor behaves like $N_q \sim |q|$ and the Fourier transform of the Jastrow parameters like $v_q \sim 1/|q|$; on the other hand, for $U > U_c^{\text{MI}}$, we have that $N_q \sim q^2$ and $v_q \sim 1/q^2$. Thus in the intermediate phase with long-range magnetic order and finite compressibility, $N_q \sim |q|$ and $v_q \sim 1/|q|$. In order to understand which is the most relevant ingredient that opens the charge gap, we calculate the structure factor N_q and the disconnected term N_q^{disc} close to Mott transition for the full variational wave function $|\Psi\rangle = \mathcal{JG}|SD\rangle$ and for another state that only contains Gutzwiller terms, i.e., $|\Psi_g\rangle = \mathcal{G}|SD\rangle$. The Slater determinant $|SD\rangle$ is independently optimized in the two cases. The results for N_q and N_q^{disc} are reported in Fig. 12 and indicate that the behavior for the two states is very similar; even the critical value U_c^{MI} for the Mott transition is the same in the two cases. Therefore, we can conclude that, in the magnetic case, the charge gap opens mainly because of

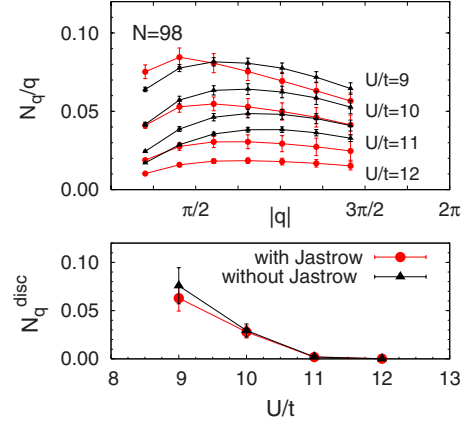


FIG. 12. (Color online) Comparison between the results obtained with the full variational wave function (full circles), containing both Gutzwiller and Jastrow terms, and the one obtained with no Jastrow factor but only the Gutzwiller projector (full triangles). N_q is shown in the upper panel and N_q^{disc} in the lower panel.

the presence of the mean-field order parameter. However, within the correlated wave function $|\Psi\rangle$, the Jastrow parameters still behave like $v_q \sim 1/q^2$ in the Mott phase.

In summary, the following scenario emerges: in the intermediate phase with antiferromagnetic order but finite compressibility, the mean-field density of state is large at the Fermi level, however, all states are localized; by increasing the interaction U , the Jastrow factor becomes stronger and, at the same time, there is a suppression of the mean-field density of states at the Fermi level; by further increasing U , a single-particle gap opens and the system becomes incompressible, see Fig. 13. We remark that the tendency toward metallicity for intermediate values of U/t is suppressed by the presence of magnetic order: this can be seen by noticing a reduced density of states at the Fermi level for $U/t \sim 8$. In fact, for small values of the interaction, the localization length is short because of the strong disorder; then it becomes larger for higher values of the interaction U due to the disorder screening and then, at the antiferromagnetic transition, it decreases again. Moreover, we notice that the single-

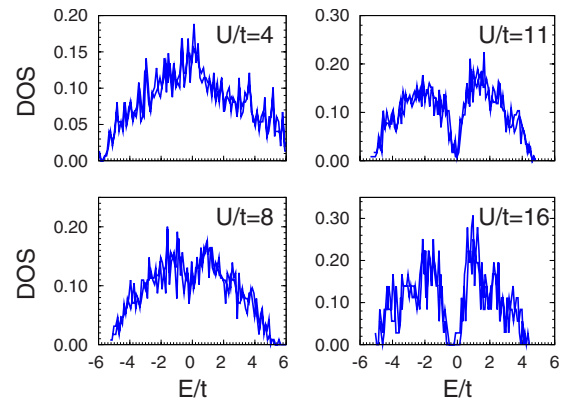


FIG. 13. (Color online) Evolution of the DOS of the auxiliary mean-field Hamiltonian as a function of the interaction U for $N=98$ sites. The case with spin-dependent on-site energies $\tilde{\epsilon}_{i,\sigma}$ is considered.

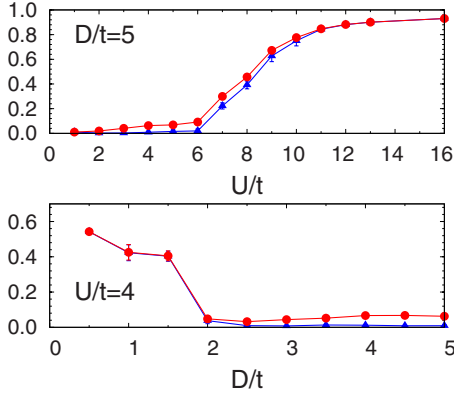


FIG. 14. (Color online) Staggered magnetization M (blue triangles) and fluctuations of the local magnetization M_L (red circles) as a function of U for disorder $D/t=5$ (upper panel) and as a function of D for $U/t=4$ (bottom panel). Calculations have been done for $N=98$ sites.

particle wave functions are more localized in the magnetic case than in the paramagnetic one, even in the regime of maximum “delocalization,” i.e., $U \sim D$. Unfortunately, a full analysis of size scaling of the localization length (by considering the inverse participation ratio, as used in Ref. 20) is very hard, because the available sizes do not allow us to reach definitive conclusions.

Let us now focus on the development of local magnetic moments in presence of the Coulomb interaction, in order to demonstrate that they may appear before the metal-insulator transition. For this issue, we consider the following quantity, which is related to the fluctuations of the local magnetization:

$$M_L = \sqrt{\frac{1}{N} \sum_i \langle m_i \rangle^2}. \quad (15)$$

In a paramagnetic state with local moments, namely, a state in which some sites have an on-site magnetization $\langle m_i \rangle \neq 0$, the total staggered magnetization is vanishing, i.e., $M=0$, while M_L is finite. On the contrary, in the antiferromagnetic phase $M_L \approx M$. Therefore, by comparing M_L and M , it is possible to have a good feeling on the presence of local moments in the ground state. In Fig. 14, we show the staggered magnetization M and M_L both for $D/t=5$ and different values of the interaction U and for $U/t=4$ and different disorder strengths D . We find that for $U > U_c^{\text{AF}} = (6.5 \pm 0.5)t$ [and for $D < D_c^{\text{AF}} = (2.5 \pm 0.5)t$] the two magnetization values are very close, while in the paramagnetic phase we observe that $M_L > M \approx 0$. This fact suggests a magnetically disordered phase in which the on-site magnetization $\langle m_i \rangle$ is finite for some sites. We identify those sites with $\langle m_i \rangle \neq 0$ as local magnetic moments. The existence of such moments can be extracted from the pattern of the on-site magnetization $\langle m_i \rangle$ (as shown in Ref. 38) or from the probability distribution of $|\langle m_i \rangle|$, see Fig. 15. Here, we observe that for small interaction values, $U/t \sim 3$, the distribution has a narrow peak in correspondence of $|\langle m_i \rangle| = 0$, however, at the same time, it has long tails indicating the presence of local moments. In this regime, the ground state is an Anderson insulator with a large

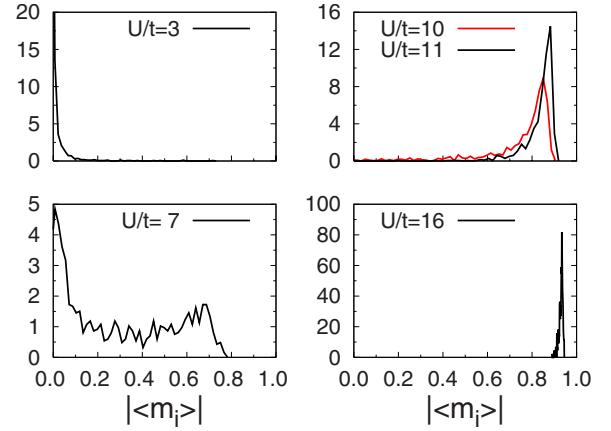


FIG. 15. (Color online) Probability distribution of the absolute value of the on-site magnetization $|\langle m_i \rangle|$ for $N=98$, $D/t=5$ and different values of the interaction U/t .

number of paramagnetic sites and $\langle n_i \rangle = 0, 1, 2$. For $U \approx U_c^{\text{AF}}$ the distribution is spread between 0 and 0.8, with a peak in correspondence of $|\langle m_i \rangle| \sim 0$. This fact highlights the coexistence of paramagnetic sites with local magnetic moments; these sites are not spatially correlated hence long-range magnetism is absent. By increasing the interaction strength, the peak at $|\langle m_i \rangle| \sim 0$ disappears and the one at $|\langle m_i \rangle| \sim 1$ becomes more pronounced; in this case, local moments eventually display the typical staggered pattern of Néel order. Nevertheless, charge excitations are still gapless and $N_q \sim |q|$. Finally, in the Mott insulating phase the distribution has a narrow peak at $|\langle m_i \rangle| = 1$.

B. Frustrating case

In the previous section, we showed that a disordered system of electrons on a square lattice undergoes a magnetic transition before becoming a Mott insulator. Therefore, the Mott insulator is generically accompanied by magnetic order. However, in disordered materials, one could expect that long-range order may be strongly suppressed, leading to a *bona-fide* Mott transition, where the incompressible phase has no magnetic order. In this sense, the presence of a next-nearest-neighbor hopping t' may help to approach the Mott phase without any spurious magnetic effects. Indeed, this kind of frustrated hopping generates, in the strong-coupling regime, a superexchange term J' that competes with the nearest-neighbor one J .

First of all, we notice that a finite frustrating ratio t'/t generates very complicated energy landscapes, with many local minima. Furthermore, in contrast to the unfrustrated model, where different local minima share very similar physical properties, here different starting points in the parameter space may give rise to rather different wave functions, especially in the intermediate and strong-coupling regimes. Concerning the starting point for the energy optimization, we will consider (i) a paramagnetic point with $\tilde{\epsilon}_{i,\uparrow} = \tilde{\epsilon}_{i,\downarrow}$, (ii) a staggered point with $\tilde{\epsilon}_{i,\sigma} = \tilde{\epsilon}_i + \sigma(-1)^{|x_i+y_i|} \delta$, and (iii) a collinear point with $\tilde{\epsilon}_{i,\sigma} = \sigma(-1)^{|x_i|}$. Notice that, in the latter case, the starting choice breaks both translational and

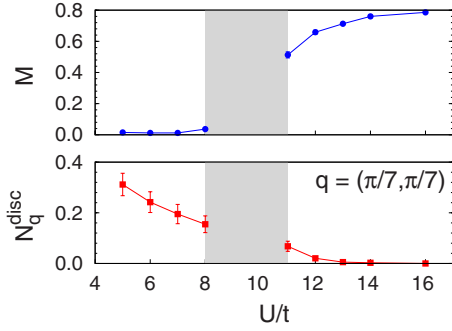


FIG. 16. (Color online) Collinear magnetization M (upper panel) and the disconnected term of the density-density correlations N_q^{disc} (lower panel) of the lowest energy solution as a function of U for $D/t=5$ and $t'/t=1$. The shaded area indicates the region where paramagnetic and magnetic solutions have similar energies.

rotational invariances, so to favor collinear magnetic order with $Q=(\pi, 0)$, which is suitable for large t'/t . Similarly, we can also consider $\tilde{\epsilon}_{i,\sigma}=\sigma(-1)^{|y_i|}$, which gives rise to a collinear order with $Q=(0, \pi)$. In all these cases, each local energy $\tilde{\epsilon}_{i,\sigma}$ (for up and down spins) is independently optimized, in order to achieve a full energy minimization.

For weak and intermediate frustrations, the outcome is rather similar to the case with $t'=0$, except for $U \sim U_c^{\text{AF}}$. For instance, for $t'/t=0.6$ and $D/t=5$, the paramagnetic Anderson insulator is stable for $U < U_c^{\text{AF}} \approx 6t$. Up to this value of the Coulomb interaction, the energy of the converged state does not depend on the choice of the starting point (as for the unfrustrated case) and there is no evidence for any nontrivial magnetic pattern. On the contrary, for $6 < U/t < 12$, different results for the staggered magnetization are found when we initialize according to (i) or (ii). In particular, the magnetization is strongly suppressed when considering a paramagnetic initial condition. These different solutions are very close in energy up to $U \approx 8t$, even though, usually, the lowest minimum shows long-range order and finite compressibility; for larger values of the interactions, i.e., $8 < U/t < 12$, the magnetic state gives definitely the best energy. By further increasing the Coulomb repulsion, namely, for $U > U_c^{\text{MI}} \approx 12t$, the system becomes a Mott insulator with Néel order at $Q=(\pi, \pi)$. These results suggest that, for a finite frustrating ratio, the magnetic transition may become weakly first order (with a regime in which there is a coexistence of different phases).

The existence of a finite region with nearly degenerate states with different magnetic properties is even more pronounced in the strong frustration regime. For $t'=t$, the solution obtained starting from (ii) gives always a higher energy with respect to (i) and (iii), demonstrating that the Néel state is clearly disadvantaged. Again, in the weakly correlated regime, i.e., $U < U_c^{\text{AF}} \approx 8t$, paramagnetic and magnetic starting points give similar energies and magnetization patterns. For $U > U_c^{\text{MI}} \approx 13t$, the ground state is a gapped insulator with $N_q^{\text{disc}}=0$, see Fig. 16. Instead, in the intermediate region, for $U_c^{\text{AF}} < U < U_c^{\text{MI}}$, the energy landscape shows different minima, which are nearly degenerate up to $U \approx 11t$, whereas, for larger interactions, the wave function with collinear order gives the best approximation for the ground state, with a clear long-range magnetic order, see Fig. 16.

The remarkable feature is that, in a wide range of Coulomb repulsions, it is possible to find low-energy states just by starting from a paramagnetic wave function. This choice gives rise to patterns in which most of the sites have a net magnetization but an overall vanishing magnetic order. For $U/t \sim 16$, these solutions are incompressible, i.e., $N_q^{\text{disc}} \sim 0$ and, therefore, may be viewed as disordered Mott insulators. By decreasing the interaction strength, these states turn compressible, still having a large number of local moments. The presence of these metastable solutions, which are almost degenerate with the magnetically ordered wave function, suggests a sort of “spin-glass” behavior. The existence of a large number of such disordered states prevents one to have a smooth convergence to the lowest energy solution, by starting from a generic configuration.

In summary, the frustrating hopping t' has two primary effects. The first one is the narrowing of the stability region of the magnetic Anderson insulator. In addition, we have evidence that the magnetic transition turns to be first order, in contrast to the unfrustrated case. The second and most important effect of a frustrating hopping term is the development of a “glassy” phase at strong couplings, where many paramagnetic states, with disordered local moments, may be stabilized. Although we do not find any evidence in favor of the stabilization of a true (nonmagnetic) Mott phase, this possibility cannot be ruled out in the whole phase diagram.

VI. CONCLUSIONS

In this paper, we have studied, by means of a variational Monte Carlo technique, zero-temperature properties of the disordered two-dimensional Hubbard model at half filling. First of all, we showed that a variational wave function is able to describe the Anderson-Mott transition without any symmetry breaking, i.e., a transition from a paramagnetic Anderson insulator to a paramagnetic Mott insulator. This is achieved thanks to long-range charge correlations induced in the wave function by a Jastrow factor. We showed that the transition can be easily detected within variational Monte Carlo by looking at the behavior of the static structure factor and of the Fourier transform of the Jastrow parameters, namely, following the same criteria for the Mott transition in a clean system. Moreover, we found that the disconnected term of the density-density correlation function, i.e., $\lim_{q \rightarrow 0} \overline{\langle n_{-q} \rangle \langle n_q \rangle}$, acts as an easily accessible order parameter for the Anderson-Mott transition. We found that electron-electron repulsion partially screens disorder: for strong interaction electrons feel an effective weak disorder potential that should imply an interaction-increased localization length. However, once the interaction exceeds a critical value, a gap opens and the model turns into a Mott insulator. From our numerical calculations, the ground state is always insulating, yet, upon increasing the strength of interaction, the localization length may have a nonmonotonous behavior when we consider the full variational wave function.

When magnetism is allowed, a compressible and magnetic Anderson insulating phase appears between the compressible paramagnetic Anderson insulator and the incompressible magnetic Mott insulator. When magnetism is not

frustrated, all transitions are likely to be continuous. On the contrary, when frustration is included by means of next-nearest-neighbor hopping, the paramagnetic to magnetic transition turns first order. Moreover, in the magnetic region, it is also possible to stabilize many paramagnetic solutions with very low energy, suggesting a glassy behavior at finite temperature. Indeed, all these paramagnetic states have local moments, i.e., magnetic sites that would contribute with a finite $-k_B \ln 2$ term to the entropy at finite temperature. The

fact that, in this simple two-dimensional model, we find local moments in the paramagnetic phase may suggest that this is a general feature of disordered systems close to a Mott transition.

ACKNOWLEDGMENT

We are particularly indebted to M. Fabrizio for enlightening discussions and for his careful reading of the manuscript.

-
- ¹N. F. Mott, Proc. Phys. Soc. London **62**, 416 (1949).
²P. W. Anderson, Phys. Rev. **109**, 1492 (1958).
³E. Abrahams, P. W. Anderson, D. C. Licciardello, and T. V. Ramakrishnan, Phys. Rev. Lett. **42**, 673 (1979).
⁴B. L. Altshuler, A. G. Aronov, and P. A. Lee, Phys. Rev. Lett. **44**, 1288 (1980).
⁵B. L. Altshuler and A. G. Aronov, Solid State Commun. **46**, 429 (1983).
⁶A. M. Finkel'stein, Z. Phys. B: Condens. Matter **56**, 189 (1984).
⁷C. Castellani, C. Di Castro, P. A. Lee, and M. Ma, Phys. Rev. B **30**, 527 (1984).
⁸T. R. Kirkpatrick and D. Belitz, Phys. Rev. B **53**, 14364 (1996).
⁹A. Georges, G. Kotliar, W. Krauth, and M. J. Rozenberg, Rev. Mod. Phys. **68**, 13 (1996).
¹⁰J. T. Chayes, L. Chayes, D. S. Fisher, and T. Spencer, Phys. Rev. Lett. **57**, 2999 (1986).
¹¹R. W. Helmes, T. A. Costi, and A. Rosch, Phys. Rev. Lett. **101**, 066802 (2008).
¹²G. Borghi, M. Fabrizio, and E. Tosatti, Phys. Rev. Lett. **102**, 066806 (2009).
¹³S. V. Kravchenko, G. V. Kravchenko, J. E. Furneaux, V. M. Pudalov, and M. D'Iorio, Phys. Rev. B **50**, 8039 (1994).
¹⁴S. V. Kravchenko and M. P. Sarachik, Rep. Prog. Phys. **67**, 1 (2004), and references therein.
¹⁵C. Castellani, C. Di Castro, and P. A. Lee, Phys. Rev. B **57**, R9381 (1998).
¹⁶A. Punnoose and A. M. Finkel'stein, Science **310**, 289 (2005).
¹⁷E. Abrahams, S. V. Kravchenko, and M. P. Sarachik, Rev. Mod. Phys. **73**, 251 (2001).
¹⁸B. L. Altshuler, D. L. Maslov, and V. M. Pudalov, Physica E (Amsterdam) **9**, 209 (2001).
¹⁹J. Huang, J. S. Xia, D. C. Tsui, L. N. Pfeiffer, and K. W. West, Phys. Rev. Lett. **98**, 226801 (2007); M. J. Manfra, E. H. Hwang, S. Das Sarma, L. N. Pfeiffer, K. W. West, and A. M. Sergent, *ibid.* **99**, 236402 (2007); S. Das Sarma, M. P. Lilly, E. H. Hwang, L. N. Pfeiffer, K. W. West, and J. L. Reno, *ibid.* **94**, 136401 (2005).
²⁰D. Heidarian and N. Trivedi, Phys. Rev. Lett. **93**, 126401 (2004).
²¹H. Shinaoka and M. Imada, J. Phys. Soc. Jpn. **78**, 094708 (2009).
²²H. Shinaoka and M. Imada, arXiv:0906.4386 (unpublished).
²³V. Dobrosavljević and G. Kotliar, Phys. Rev. Lett. **78**, 3943 (1997).
²⁴D. Tanasković, V. Dobrosavljević, E. Abrahams, and G. Kotliar, Phys. Rev. Lett. **91**, 066603 (2003).
²⁵V. Dobrosavljević, A. A. Pastor, and B. K. Nikolić, Europhys. Lett. **62**, 76 (2003).
²⁶K. Byczuk, W. Hofstetter, and D. Vollhardt, Phys. Rev. Lett. **94**, 056404 (2005).
²⁷K. Byczuk, W. Hofstetter, and D. Vollhardt, Phys. Rev. Lett. **102**, 146403 (2009).
²⁸E. Z. Kuchinskii, I. A. Nekrasov, and M. V. Sadovskii, Sov. Phys. JETP **106**, 581 (2008).
²⁹P. J. H. Denteneer, R. T. Scalettar, and N. Trivedi, Phys. Rev. Lett. **83**, 4610 (1999).
³⁰M. Ulmke, V. Janis, and D. Vollhardt, Phys. Rev. B **51**, 10411 (1995).
³¹M. Ulmke and R. T. Scalettar, Phys. Rev. B **55**, 4149 (1997).
³²V. Janis, M. Ulmke, and D. Vollhardt, Europhys. Lett. **24**, 287 (1993).
³³M. Milovanović, S. Sachdev, and R. N. Bhatt, Phys. Rev. Lett. **63**, 82 (1989).
³⁴M. C. O. Aguiar, V. Dobrosavljević, E. Abrahams, and G. Kotliar, Phys. Rev. B **71**, 205115 (2005).
³⁵M. C. O. Aguiar, V. Dobrosavljević, E. Abrahams, and G. Kotliar, Phys. Rev. B **73**, 115117 (2006).
³⁶E. Miranda and V. Dobrosavljević, Phys. Rev. Lett. **86**, 264 (2001).
³⁷E. C. Andrade, E. Miranda, and V. Dobrosavljević, Phys. Rev. Lett. **102**, 206403 (2009).
³⁸M. E. Pezzoli, F. Becca, M. Fabrizio, and G. Santoro, Phys. Rev. B **79**, 033111 (2009).
³⁹S. Sorella, Phys. Rev. B **71**, 241103 (2005).
⁴⁰D. Belitz, A. Gold, W. Gotze, and J. Metzger, Phys. Rev. B **27**, 4559 (1983).
⁴¹M. Capello, F. Becca, M. Fabrizio, S. Sorella, and E. Tosatti, Phys. Rev. Lett. **94**, 026406 (2005).
⁴²M. Capello, F. Becca, M. Fabrizio, and S. Sorella, Phys. Rev. Lett. **99**, 056402 (2007); Phys. Rev. B **77**, 144517 (2008).
⁴³I. F. Herbut, Phys. Rev. B **63**, 113102 (2001).